IOP Publishing Phys. Scr. 98 (2023) 075106 https://doi.org/10.1088/1402-4896/acdda5

Physica Scripta

RECEIVED
23 February 2023

REVISED
17 May 2023

ACCEPTED FOR PUBLICATION
12 June 2023

PUBLISHED
23 June 2023

PAPER

The effect of intrinsic decoherence on the dynamics of an Ξ-type qutrit system interacting with a coherent field

A-S F Obada[1], M Hashem[2], M M Elkhateeb[2] and S-E A Rizk[2]

[1] Faculty of Science, Al-Azhar University, Nasr City, Cairo 11884, Egypt
[2] Faculty of Science, Assiut University, Assiut 71516, Egypt

E-mail: m3tz@aun.edu.eg

Keywords: three-level atom, E-type, intrinsic noise, decoherence, coherent field

Abstract

This paper solves milburn's intrinsic noise (IN) model for a 3-level atom of an Ξ-type interacting with a coherent cavity field via multiphoton transitions. Therefore, the effects of the intrinsic noise and the multi-photon interactions are investigated for some quantum phenomena, such as total correlation, entanglement, and atomic inversion. In general, we found that the collapse-revival phenomenon occurs during the oscillatory behaviour of atomic population dynamics. In addition, the birth-death phenomenon is observed in the negativity dynamics. Entropy, negativity, and mutual information have various dynamics. It is found that, as the entropy increases, the negativity and mutual information diminish to stationary levels. When intrinsic noise is considered, all the phenomena of atomic inversion, entropies, negativity and mutual information exhibit high sensitivity to high intrinsic noise values, except the mutual information dynamics, which is more resistant than that of the other quantifiers.

1. Introduction

In 1963, the Jaynes-Cummings model (JCM) was introduced as the initial approach to studying quantum systems composed of a two-level atom interacting with a single quantized cavity mode [1]. The JCM has since been the subject of numerous theoretical investigations [2] as well as experimental studies [3–6]. Over the past few decades, this approach has been extended to encompass diverse quantum systems, exploring various aspects such as photon transitions, intensity-dependent couplings, Stark shift, and Kerr non-linearity [7–11].

One notable extension of the JCM involves the consideration of three-level atoms in different configurations (Λ, V, and Ξ) interacting with one- or two-mode field(s) within a cavity. Researchers have extensively examined the interaction between a three-level atom and a one- or two-mode cavity field [12].

Furthermore, investigations have explored three-level atom models, incorporating additional elements such as multiphoton transitions, field-dependent coupling constants, Kerr-like mediums, and non-correlated two-mode fields [9–16]. Advancements in experimental techniques have furthered the understanding of such systems, particularly in the case of trapped ions [17], cooper-pair boxes [18, 19] and flux qubits [20].

Quantum information processing offers various avenues of implementation for three-level atom systems, also known as qutrits [21–23]. The exploration of nonlinear interactions between multilevel atomic systems and electromagnetic cavity fields has greatly advanced our understanding of quantum coherence, entanglement, and the loss of purity [24, 25]. These quantum phenomena have emerged as crucial research areas due to their fundamental significance in quantum information processing [26]. Thus far, our focus has primarily been on studying the dynamics of closed quantum systems, where no unwanted interactions with the external environment occur. However, in real-world scenarios, unwanted interactions with the outside world pose challenges. The existence of such noisy processes necessitates a comprehensive understanding and effective management for the development of practical quantum information processing systems [27].

Quantum coherence in quantum systems is influenced by two key factors arising from their interaction with the environment. The first factor is the loss of entanglement or coherence, which occurs due to the unitary

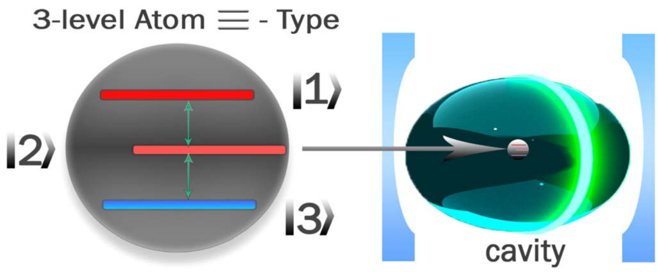

Figure 1. Quasi model of Ξ-type 3-level atom.

interaction between the quantum system and the cavity field [28]. The second factor is the decoherence or decay of quantum coherence resulting from the interaction between the quantum system and the surrounding reservoir [29]. Overcoming the challenges posed by these disruptive factors is a significant hurdle in quantum information processing.

In this study, we investigate the efficacy of a particular approach known as IN (Interaction with the Environment) for three-level atoms of the Ξ-type. IN is recognized as a crucial method for simulating decoherence phenomena. It reveals its effects as the system evolves, leading to the automatic disappearance of coherence and eventual collapse of the quantum system [30]. Theoretically examine the dynamics of IN in a three-level atom of the Ξ-type, we employ the Milburn equation as our primary mathematical framework for describing the dynamics of open quantum systems. Specifically, we consider a scenario where the qutrit is initially in the upper state and interacts with a coherent field through multi-photon transitions. Subsequently, we obtain the density matrix and present a numerical simulation to demonstrate the impact of IN and photon multiplicity on various quantum effects.

The structure of this paper is as follows: section 2 provides the analytical solution for the IN model. In section 3, we present the quantum effect quantifiers along with their corresponding numerical simulations. Finally, in section 4, we summarize the key findings obtained from this research.

2. Physical model

In this section, we introduce the Ξ-type three-level atom configuration, where the energy levels are labeled as follows: $|1\rangle$ represents the upper state, $|2\rangle$ corresponds to the middle level, and $|3\rangle$ represents the ground state (refer to figure 1). In the case of resonance, the interaction Hamiltonian of the system, under the assumption of the rotating wave approximation (RWA), can be expressed as follows:

$$\hat{H}_I = \lambda_1(a^k|1\rangle\langle 2| + a^{\dagger k}|2\rangle\langle 1|) + \lambda_2(a^k|2\rangle\langle 3| + a^{\dagger k}|3\rangle\langle 2|) \tag{1}$$

where $a^\dagger$ and a represent the creation and annihilation operators of the field, respectively. The parameter k denotes the photon multiplicity. The notation $|m\rangle\langle n|(m, n = 0, 1, 2, 3)$ signifies the atomic ladder operator connecting the levels of the atom. Additionally, $\lambda_r(r = 1, 2)$ represents the coupling strength between specific atom levels, denoted as λ_1 for the transition $|1\rangle \leftrightarrow |2\rangle$ and λ_2 for the transition $|2\rangle \leftrightarrow |3\rangle$).

The Milburn equation [31] is a widely recognized equation that describes the dynamics of intrinsic decoherence (IN) in quantum systems. It captures the impact of the unitary interaction between the cavity and the qutrit, which leads to the manifestation of IN. The specific form of the Milburn equation for this model is as follows:

$$\frac{d\hat{\rho}}{dt} = -i[\hat{H}, \hat{\rho}] - \gamma(\hat{H}^2\hat{\rho} - 2\hat{H}\hat{\rho}\hat{H} + \hat{\rho}\hat{H}^2), \tag{2}$$

where γ is the parameter of IN.

In order to find the solution to equation (2),we take into account the initial conditions where the field is prepared in a coherence state and the atom is in an excited state. Hence, the initial density matrix, denoted as $\hat{\rho}(0)$ can be expressed as follows:

$$\hat{\rho}(0) = \sum_{m,n} q_m q_n^*|1, m\rangle\langle 1, n|, \qquad q_m = e^{\frac{-N}{2}}\frac{\alpha^m}{\sqrt{m!}} \tag{3}$$

where $N = |\alpha|^2$ refer to the mean number of photons.

Our problem can be mathematically formulated in Hilbert space, which is spanned by the basis $\{|\Phi_1\rangle = |1, m\rangle, |\Phi_2\rangle = |2, m + k\rangle, |\Phi_3\rangle = |3, m + 2k\rangle\}$. The dressed states $|\Psi_i^m\rangle (i = 1, 2, 3)$ satisfy the eigenvalue problem

$\hat{H}|\Psi_i^m\rangle = E_i^m|\Psi_i^m\rangle$ and are given by:

$$\begin{bmatrix}|\Psi_1^m\rangle\\|\Psi_2^m\rangle\\|\Psi_3^m\rangle\end{bmatrix} = \xi_m\begin{bmatrix}-v & 0 & u\\ \frac{u}{\sqrt{2}} & \frac{1}{\xi_m\sqrt{2}} & \frac{v}{\sqrt{2}}\\ \frac{u}{\sqrt{2}} & \frac{-1}{\xi_m\sqrt{2}} & \frac{v}{\sqrt{2}}\end{bmatrix}\begin{bmatrix}|\Phi_1\rangle\\|\Phi_2\rangle\\|\Phi_3\rangle\end{bmatrix}, \tag{4}$$

where $u = \lambda_1\sqrt{\frac{(m+k)!}{m!}}$, $v = \lambda_2\sqrt{\frac{(m+k+2)!}{(m+2)!}}$ and $\xi_m = \frac{1}{\sqrt{u^2+v^2}}$, and the corresponding eigenvalues are

$$E_1^m = 0, \qquad E_{2,3}^m = \frac{\pm 1}{\xi_m}. \tag{5}$$

In this context, we will consider two cases: one-photon transition ($k = 1$) and two-photon transition ($k = 2$), where $\lambda_1 = \lambda_2 = \lambda$ in both cases.

Now, using equation (2), the time evolution operator for the states can be expressed as follows:

$$\hat{X}_{rs}^{mn} = \Omega_{rs}^{mn}|\Psi_r^m\rangle\langle\Psi_s^n| \tag{6}$$

where $\Omega_{rs}^{mn} = e^{[-i(E_r^m - E_s^n) - \gamma(E_r^m - E_s^n)^2]t}$.

Now, from equation (2) and (6), the density operator of the system can be expressed as follows:

$$\hat{\rho}(t) = \sum_{m,n=0}^{\infty}\sum_{i,j=1}^{3}(\xi_m\xi_n)^2 q_m q_n^* \boldsymbol{\Theta}_{ij}, \tag{7}$$

where $\boldsymbol{\Theta}_{ij}$ are:

$$\begin{aligned}
\boldsymbol{\Theta}_{11} &= (v_m v_n)^2\Omega_{11}^{mn} + \frac{1}{2}[(v_m u_n)^2 a_+ + (u_m v_n)^2 a_+^*] + \frac{1}{4}(u_m u_n)^2 b_+,\\
\boldsymbol{\Theta}_{12} &= \frac{1}{4\xi_n}[2u_n v_m^2 a_- + u_n u_m^2(b_- - 2c_-)],\\
\boldsymbol{\Theta}_{13} &= \frac{u_n v_n v_m^2}{2}(-2\Omega_{11}^{mn} + a_+) + \frac{u_n v_n u_m^2}{4}(-2a_+^* + b_+),\\
\boldsymbol{\Theta}_{22} &= \frac{u_m u_n}{4\xi_m\xi_n}[b_+ - 2c_+],\\
\boldsymbol{\Theta}_{23} &= \frac{u_m u_n v_n}{4\xi_m}[b_- - 2a_-^*],\\
\boldsymbol{\Theta}_{33} &= \frac{(u_m v_m)(u_n v_n)}{4}[4\Omega_{11}^{mn} - 2(a_+ + a_+^*) + b_+],
\end{aligned}$$

where:

$$\begin{aligned}
a_\pm &= \Omega_{12}^{mn} \pm \Omega_{13}^{mn}, \qquad (a_\pm)^* = \Omega_{21}^{mn} \pm \Omega_{31}^{mn},\\
b_\pm &= (\Omega_{22}^{mn} \pm \Omega_{33}^{mn}) + c_\pm, \; c_\pm = \Omega_{23}^{mn} \pm \Omega_{32}^{mn}.
\end{aligned}$$

And $\boldsymbol{\Theta}_{ij} = \boldsymbol{\Theta}_{ji}^* \forall\, i, j = 1, 2, 3.$

In the following section, we will run a numerical approach supported by some figures to investigate the effect of the IN on some quantum phenomena.

3. Numerical simulation for some quantum indicators

In this section, we will apply the solution obtained from the previous section in a numerical context to explore the effect of some physical parameters, including intrinsic decoherence (IN), photon multiplicity, and mean photon number, on various quantum phenomena. Specifically, we will investigate their effects on atomic inversion, total correlation, and quantum coherence. By conducting numerical simulations, we aim to gain a deeper understanding of how these parameters influence the behavior of the system and the resulting quantum effects.

3.1. Atomic population

The phenomenon of atomic population inversion plays a crucial role in the field of laser science. To comprehend this phenomenon, it is necessary to gasp the interaction between the Ξ-qutrit and the cavity-field, which is analogous to how light interacts with matter in a laser system [32]. Additionally, the phenomenon has a vital role in quantum meteorology, which can be used to create highly accurate atomic clocks [33]. It can also be used to achieve highly sensitive spectroscopic measurements [34]. The disparity between the probabilities of finding an

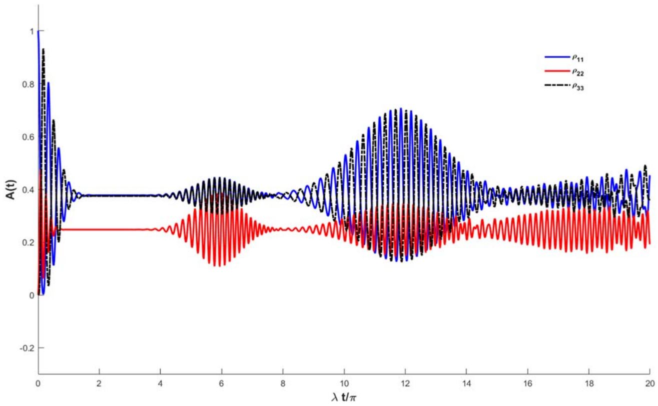

Figure 2. The atomic population for each level with N(mean photon number)=16 and $\gamma = 0$ (IN-parameter).

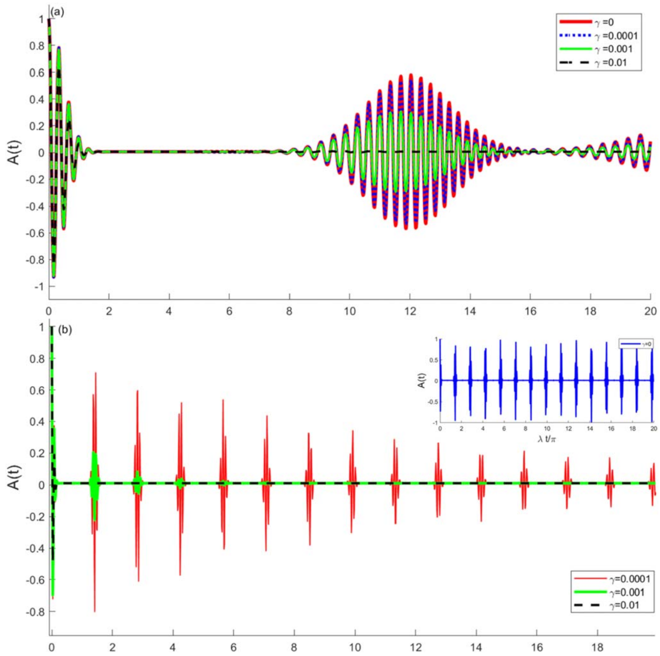

Figure 3. The atomic inversion $A(t)$ dynamic for N(mean photon number)=16, for the different values of γ (IN-parameter) are: 0 (blue curve), 0.0001 (red curve), 0.001 (green dashed curve, and 0.01 (black curve), with k (the photon multiplicity)=1 in (a) and $k = 2$ in (b).

atom in its lowest and highest energy states is referred to as atomic population inversion. In our model, the formula for atomic inversion can be expressed as follows [35, 36]:

$$A(t) = \langle \Phi_1 | \hat{\rho}(t) | \Phi_1 \rangle - \langle \Phi_3 | \hat{\rho}(t) | \Phi_3 \rangle, \tag{8}$$

$$|\Phi_1\rangle = |1, m\rangle, \qquad |\Phi_3\rangle = |3, m + 2k\rangle.$$

Figure 2 depicts the dynamic behavior of the atomic population in each level, which motivates us to define the atomic inversion as shown in equation (8).

Figure 3 illustrates the dynamical behavior of $A(t)$ for different values of IN and k-photon transitions, with $N = 16$. The graphs demonstrate that the atomic inversion undergoes collapses and revivals, this refers to the consistency and variability of the qutrit energy transfer. The revival oscillating between its extreme values (± 1) around $A(t) = 0$. The oscillation occurs around zero because a pure state is considered. As in [30], a comparison between mixed and pure states was set up, and it was noticed that in the case of a mixed state, the oscillation of $A(t)$ shifted up to a certain point. As well, during the time-independent intervals when the population inversion is zero (collapse intervals) or constant, there is no energy transmission and the qutrit remains stable in a superposition state of the upper and lower states.

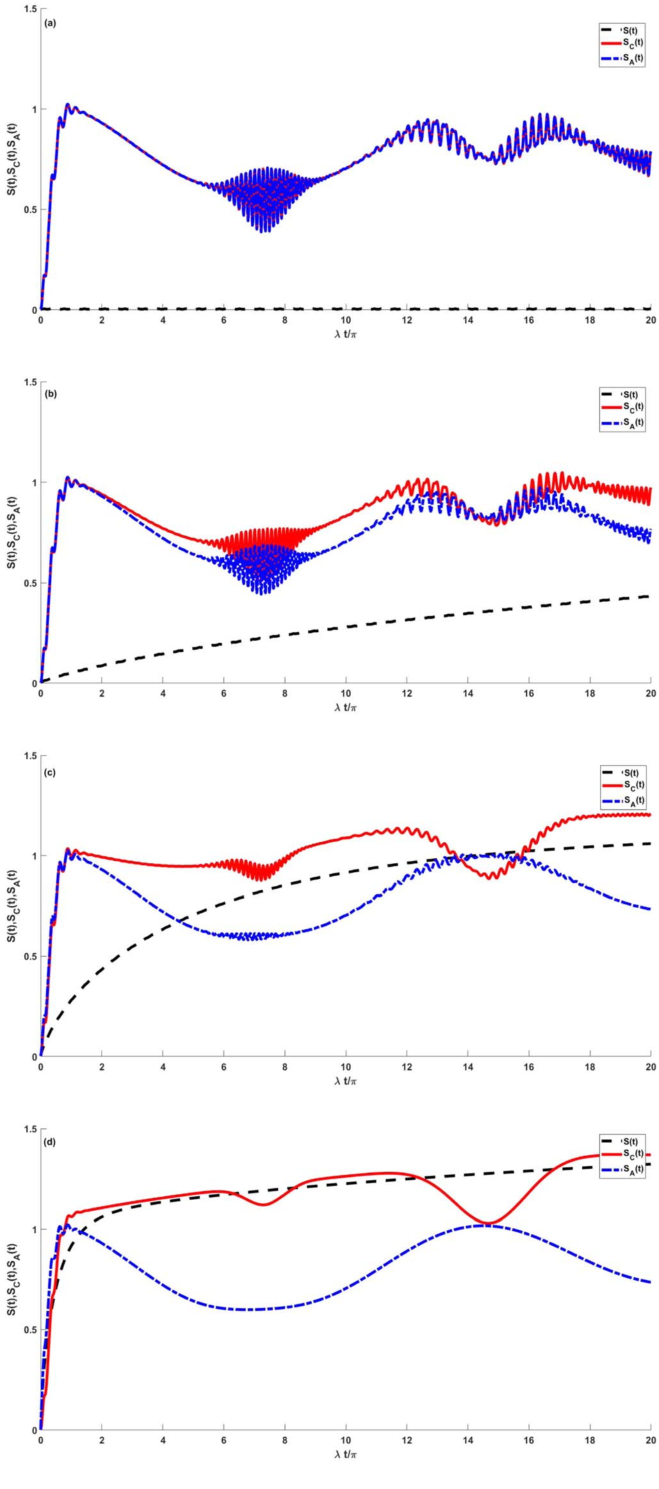

Figure 4. The dynamical behaviour of S(t) (black dashed curves), $S_A(t)$ (blue centred curves) and $S_C(t)$(red curves) with $N = 25$ and one photon transition (i.e $k = 1$) for various values of γ 0,0.0001,0.001 and 0.01 respectively in a,b,c and d.

In figure 3(a), for $k = 1$, $A(t)$ exhibits regular behavior in the absence of intrinsic noise, and the collapse and revival phenomenon is performed well. However, in the presence of IN with small values, such as $\gamma = 0.0001$, $A(t)$ retains its oscillatory behavior, but the amplitude of $A(t)$ is smaller than when the noise is absent. Figure 3(a) also shows that as IN increases, the amplitude of $A(t)$ decreases until decay at $\gamma = 0.01$(black-dashed line). The presence of intrinsic noise (IN) in atomic clocks can lead to a reduction in their accuracy by causing the atomic population inversion to decay over time [33]. This is consistent with the theoretical study of the effect of IN on the dynamic behavior of $A(t)$, as shown in figure 3.

Figure 3(b): compared to the scenario when $k = 2$, it shows that the regular oscillatory behavior of $A(t)$ and its amplitude appears over a long range of time, but each amplitude decreases over time. Additionally, the

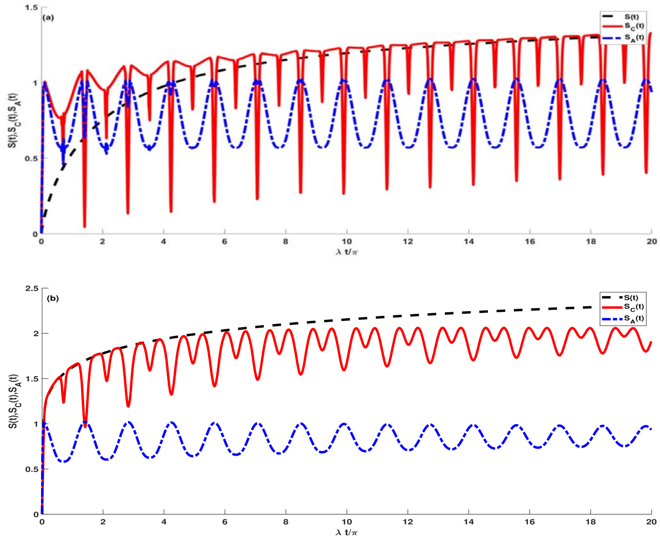

Figure 5. As figure 4 but for two photon transitions ($k = 2$).

phenomenon of collapse and revivals is very sensitive to IN. As shown in the inset figure, when IN is ignored, $A(t)$ maintains its oscillatory behavior with no damping over the evolution of time. However, when IN is taken into account, $A(t)$ gradually loses its height while keeping its oscillatory behavior by increasing the IN.

Overall, the precise dynamics of the atomic population in the presence of IN can be influenced by a variety of factors, including the strength of the coupling between the system and its environment, the nature of the noise, and the initial state of the system.

3.2. Entropy

In any system, there are two factors that may be responsible for purity loss:

- The unitary interaction, which can cause purity loss (or coherence loss) from the perspective of one of the subsystems during the process, typically referred to as entanglement.
- The interaction of any subsystem with the environment, which can also cause purity loss. This phenomenon is known as coherence loss and is generated by the environment.

The Von Neumann entropy is a quantifier used to measure the degree of purity of a state represented by the density operator, $\hat{\rho}(t)$.

$$S(\hat{\rho}(t)) = -\mathrm{Tr}(\rho \log \rho), \tag{9}$$

if $\{q_i\}$ are the eigenvalues of $\hat{\rho}(t)$, then equation(9) reads,

$$S(t) = -\sum_{i=1}^{\infty} q_i \log q_i \tag{10}$$

Now, the entropies of a sub-system (atom and cavity-field) are give by:

$$S_j(t) = -\sum_i r_i^j \log r_i^j \qquad j = A,\, C \tag{11}$$

And $\{r_i^j\}$ are the eigenvalues of the reduced density operator $\hat{\rho}^j(t)$.

Some properties of $S(\rho)$:-

(1) It is a non-negative operator, meaning that $S(t) \geqslant 0$.

(2) It satisfies the triangle inequality known as the Araki-Lieb inequality [37]:

$$|S_A(t) - S_C(t)| \leqslant S(t) \leqslant S_A(t) + S_C(t).$$

(3) The minimum value of $S(t)$ is zero.

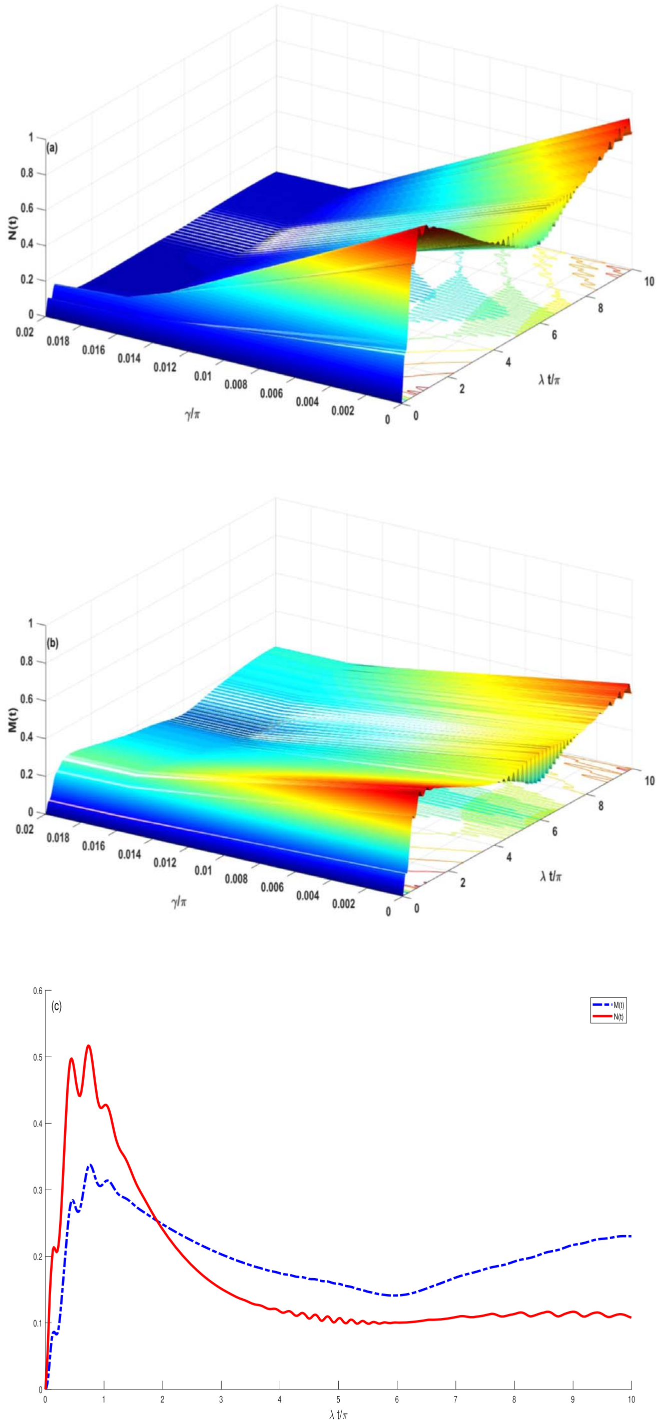

Figure 6. The dynamic behaviour of $N(t)$ and $M(t)$. The 3D-figures are plotted with respect to the different values for IN and with $N = 16$ with $k = 1$ in (a,b). $M(t)$, $N(t)$ are shown in 2D figures as line-centered curves and solid curves, respectively. with $\gamma = 0.01\lambda$ and $k = 1$.

(4) If $S(t) = 0$, *then*$S_A(t) = S_C(t)$, and this occurs only if the system is in a pure state and closed (i.e $\gamma = 0$).
Several related works have also explored the concept of entropy in the context of quantum systems, including [38, 39].

Figure 4 illustrates the entropies for the qutrit (initially in a pure and excited state), cavity field (initially in a coherent state with a mean photon-number N = 25), and total entropy, in the order of $S_A(t)$, $S_C(t)$ and $S(t)$. The purpose of the figure is to investigate the effect of different values of the intrinsic noise (IN) on the dynamical behavior of the entropies. Figure 4 (a) represents the optimal case of the absence of the IN. This observation is consistent with the properties of $S(\rho)$ presented in this section, namely that $S_A(t) = S_C(t)$ and $S(t) = 0$ in case of

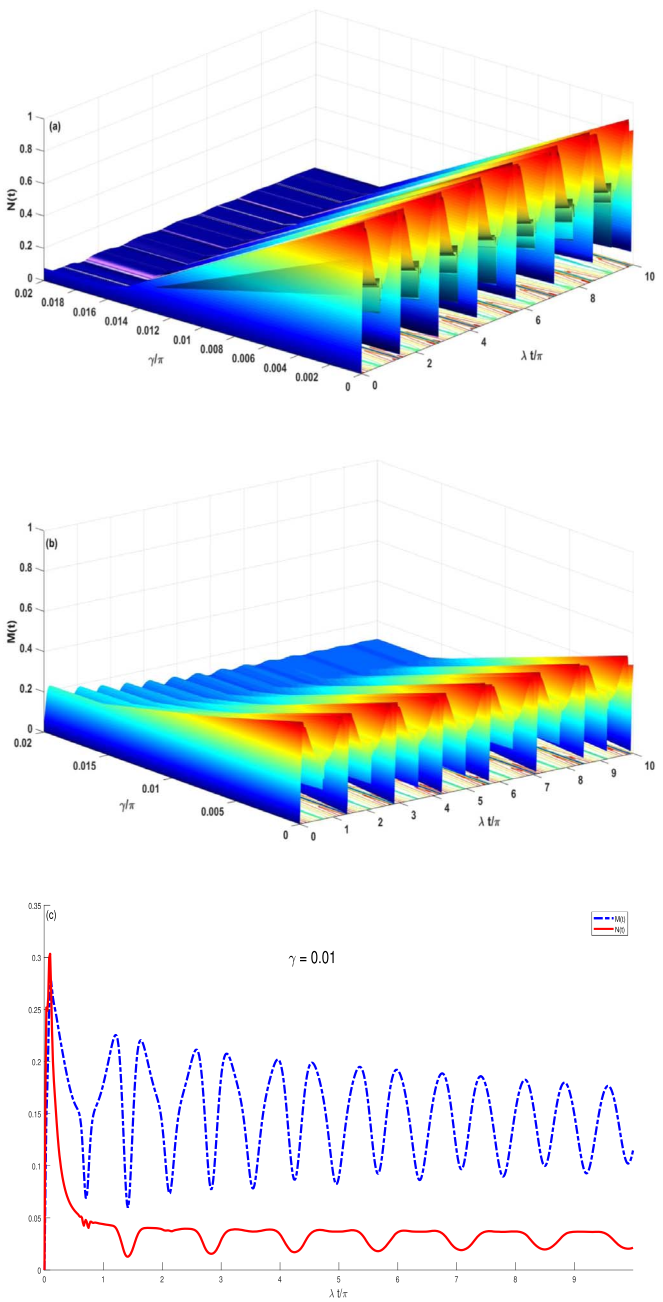

Figure 7. As the same data of figure 6, but with $k = 2$.

$\gamma = 0$. Figure 4(a) is considered the reference case for this simulation and provides critical information: $S_A(t)$ and $S_C(t)$ exhibit the same behavior, and all three entropy functions start from zero, which agrees with the theoretical simulation. Furthermore, $S(t)$ should satisfy the Araki-Lieb inequality. Figure 4 (b) depicts the behavior of the entropy functions in the presence of a small value for IN, which results in some changes to the graph.

One of the observed changes is that S_A and S_C exhibit the same oscillatory behavior, but $S_A \leqslant S_C$. Furthermore, the difference between S_C and S_A causes the total entropy to grow dramatically, which is consistent with the Araki-Lieb inequality. In figure 4(c), when the rate of IN is increased, the entropy functions remain at zero. However, the oscillatory behavior in S_A significantly declines, while S_C remains stable. In figure 4(d),it is shown that when IN is large, the oscillatory behavior in S_A and S_C is washed out.

Figure 5 depicts the evolution of the entropy functions S_A, S_C and S with IN and two photon transitions ($k = 2$). From the comparison with figure 4, we can deduce that the regularity of the oscillating behaviour is dependent on photon multiplicity. In the case of two photon transitions ($k = 2$), the initial purity of the entropy is more brittle than the case of single photon transition ($k = 1$).

3.3. Negativity and Mutual information

Here, we will investigate two important measures for correlation and entanglement, the negativity and the mutual information; We use the negativity to investigate the entanglement between the qutrit and cavity field under the influence of photon multiplicity in the presence of intrinsic noise, but the mutual information is used for studying the total correlation.

1. Negativity: is a measure of entanglement, which is easy to compute by computing the norm ($\|.\|$) of the matrix ($\hat{\rho}(t)^T$), which is generated by applying partial transpose on density matrix $\hat{\rho}(t)$ [40]. Hence, the mathematical form is given by:

$$N(t) = \frac{\|\hat{\rho}(t)^T\| - 1}{2}. \tag{12}$$

If $N(t) = 1$, this is an indicator to maximum entanglement. Moreover, if $N = 0$, This refers to disentanglement between the qutrit and the cavity.

2. Quantum mutual information (QMI): is a measure of total correlation, which is given by [41]:

$$M(t) = \frac{1}{4}\left[\left(\sum_i S_i(t)) - S(t\right)\right] \qquad i = A,\, C \tag{13}$$

The entanglement between the qutrit and the cavity is indicated by $N(t)$, while the total correlation, which carries both classic and quantum information, is described by $M(t)$. For better understanding for the behavior of these measures (negativity and QMI), it is important to analyze their dynamics.

The dynamics of $N(t)$ and $M(t)$ reflect the changes in the degree of entanglement and total correlation between the qutrit and the cavity field under different conditions. The behavior of $N(t)$ and $M(t)$ can be described as irregular oscillations. The values of $N(t)$ exhibit a decrease when the IN parameter takes on different values, which may indicate a separable state or disentanglement between the qutrit and the cavity (see figures 6(a), (c)). In contrast, $M(t)$ shows some stability against the IN for different values (see figures 6(b), (c)). We display the behavior of $M(t)$ and $N(t)$ for two distinct values of k, where $k = 1$ in figure 6 and $k = 2$ in figure 7. Specifically, figures 6(a), (b) and 7(a), (b) show the behavior of $M(t)$ and $N(t)$ under the effect of different values of the IN parameter, while figures 6(c) and 7(c) show their behavior in the case of $\gamma = 0.01\lambda$.

For $k = 2$, $M(t)$ and $N(t)$ exhibit the same behavior, but the oscillatory pattern has more regularity than in the case of $k = 1$. When $\gamma = 0$ or is nearly equal to zero, the negativity at some points on the time scale suddenly goes to zero or nearly approaches zero value, and it also shows sudden growth (see figures 7(a), (c)). This phenomenon is known as the sudden birth and death of entanglement [42, 43]. Moreover, $M(t)$ resists the influence of an increasing IN rate in the case of $k = 2$, as shown in figure 7(b). However, when we compare figure 6(c) (k= 1) and figure 7(c) ($k = 2$), we observe that at $k = 1$, $M(t)$ the dynamic appears more stable than at $k = 2$. The entanglement in the case of $k = 2$ deteriorates faster than in the case of $k = 1$. Additionally, at the beginning of the behavior, we observe an interference between the two curves, indicating an entanglement area that is destroyed more rapidly than in the case of $k = 1$ However, in the presence of IN with different values, $M(t)$ exhibits some stability against the IN, unlike $N(t)$, and this indicates that the effect of internal noise causes the model to lose some of its quantum properties and brings it closer to classical bounds (see figures 6(b), (c)).

4. Conclusion

In this article, we studied an Ξ-type three-level atom resonantly interacting with a cavity field. The field is initially prepared in a coherent state, and the atom is in its upper state. Our focus is on studying the decoherence, which is presented through an analytical solution for the Milburn equation. We aim to understand the effect of physical parameters, such as photon multiplicity and intrinsic noise, on atomic inversion, quantum coherence through entropy, entanglement using negativity, and correlation through mutual information. We observe that the collapse-revival phenomenon is highly sensitive to intrinsic noise, and the oscillations and amplitudes of the atomic inversion curves depend on photon multiplicity. The entropy functions exhibit highly dependent behaviour on photon transitions and intrinsic noise. The regularity of the oscillatory behaviour and the amplitude of the oscillations show high sensitivity to these parameters. While the cavity and qutrit-cavity entropies rise without limitation, allowing the Araki-Lieb inequality, the stationary value of the qutrit entropy remains fixed. Moreover, we find that the physical properties of the unitary interaction, intrinsic noise, and photon multiplicity affect the produced qutrit-cavity entanglement and total correlation. The negativity depends on the intrinsic noise and the number of photon transitions, while the mutual information shows some robustness against the intrinsic noise. However, the behaviour of mutual information shows a dependency on the photon multiplicity parameter.

Data availability statement

All data that support the findings of this study are included within the article (and any supplementary files).

ORCID iDs

M M Elkhateeb https://orcid.org/0000-0003-3404-5808

References

[1] Jaynes E T and Cummings F W 1963 *Proceedings of the IEEE* 51 89
[2] Shore B W and Knight P L 1993 *J. Mod. Opt.* **40** 1195
[3] Feng Z-B, Yan R-Y and Zhou Y-Q 2013 *Quantum Inf. Process.* **12** 1429
[4] Gharamaleki A H, Kevin A and Tavakoli Ghazi Jahani M A 2019 *Eur. Phys. J.* D **73** 1
[5] Jelezko F, Gaebel T, Popa I, Gruber A and Wrachtrup J 2004 *Phys. Rev. Lett.* **92** 076401
[6] Mishra S K, Chotorlishvili L, Rau A and Berakdar J 2014 *Phys. Rev.* A **90** 033817
[7] Korashy S, Abdel-Rady S and Osman A-N A 2017 *Quant. Inf. Rev.* **5** 9
[8] Yoo H-I and Eberly J H 1985 *Phys. Rep.* **118** 239
[9] Mohamed A-B, Elkhateeb M, Hashem M and Obada A-S 2022 *Alexandria Engineering Journal* **61** 2348
[10] Mohamed A-B, Elkhateeb M, Hashem M, Obada A-S and Eleuch H 2020 *Mod. Phys. Lett.* A **35** 2050287
[11] Abdel-Aty M 2000 *J. Phys. B: At. Mol. Opt. Phys.* **33** 2665
[12] Li X-S *et al* 1987 *Phys. Rev.* A **36** 5209
[13] Abdel-Hafez A, Obada A and Ahmad M 1987 *Physica A* **144** 530
[14] Abdel-Hafez A, Abu-Sitta A and Obada A-S 1989 *Physica A* **156** 689
[15] Abdel-Aty M 2001 *Laser Phys.* **11** 871
[16] Obada A F, Hanoura S and Eied A 2013 *Laser Phys.* **23** 055201
[17] Leibfried D, Blatt R, Monroe C and Wineland D 2003 *Rev. Mod. Phys.* **75** 281
[18] Irish E K and Schwab K 2003 *Phys. Rev.* B **68** 155311
[19] Wallraff A, Schuster D I, Blais A, Frunzio L, Huang R-S, Majer J, Kumar S, Girvin S M and Schoelkopf R J 2004 *Nature* **431** 162
[20] Chiorescu I, Bertet P, Semba K, Nakamura Y, Harmans C and Mooij J 2004 *Nature* **431** 159
[21] Zhang X, Ding X and Ge X 2020 *Quantum Inf. Process.* **19** 1
[22] Lin J, Hou K, Zhu C and Yang Y 2019 *Phys. Rev.* A **99** 053850
[23] Chien W-C, Hsieh Y-L, Chen C-H, Dubyna D, Wu C-S and Kuo W 2019 *Opt. Express* **27** 36088
[24] Heshami K, England D G, Humphreys P C, Bustard P J, Acosta V M, Nunn J and Sussman B J 2016 *J. Mod. Opt.* **63** 2005
[25] Obada A F, Hessian H and Mohamed A A 2009 *J. Phys. A: Math. Theor.* **43** 025305
[26] Mohamed A, Eleuch H and Ooi C 2019 *Sci. Rep.* **9** 1
[27] Nielsen M A and Chuang I 2002 *Quantum Computation and Quantum Information* (American Journal of Physics 70, 558–559: AIP Publishing) (https://doi.org/10.1119/1.1463744)
[28] Obada A F, Mohamed A A, Hashem M and Elkhateeb M 2020 *Laser Phys.* **30** 055203
[29] Ikram M, Li F-l and Zubairy M S 2007 *Phys. Rev.* A **75** 062336
[30] Obada A F, Mohamed A A, Hashem M and Elkhateeb M 2020 *Phys. Scr.* **95** 085101
[31] Milburn G 1991 *Phys. Rev.* A **44** 5401
[32] Svelto O and Hanna D C 1998 *Principles of Lasers* (Berlin: Berlin) Vol 4, pp 365–418
[33] Giovannetti V, Lloyd S and Maccone L 2011 *Nat. Photonics* **5** 222
[34] Sturge M D 1970 *Phys. Rev. Lett.* **24** 775
[35] Cohen-Tannoudji C, Diu B and Laloe F 1998 *Quantum Mechanics* (New York: Wiley) Vol. 1
[36] Obada A-S, Ahmed M, Salah A and Farouk A M 2016 *J. Mod. Opt.* **63** 2315
[37] Araki H and Lieb E H 1970 *Commun. Math. Phys.* **18** 160
[38] Rudnicki Ł, Puchała Z and Życzkowski K 2014 *Phys. Rev.* A **89** 052115
[39] Ming F, Wang D, Fan X-G, Shi W-N, Ye L and Chen J-L 2020 *Phys. Rev.*A **102** 012206
[40] Vedral V, Plenio M B, Rippin M A and Knight P L 1997 *Phys. Rev. Lett.* **78** 2275
[41] Walczak Z 2009 *Phys. Lett.* A **373** 1818
[42] Yu T and Eberly J 2004 *Phys. Rev. Lett.* **93** 140404
[43] Yu T and Eberly J 2009 *Science* **323** 598